evidence suggests that CR2 binds to C3d and EBV gp350/220 with overlapping but distinct sites (*28*) and involves S16 and Y68. These residues mapped on the CR2 surface are separated from the area that interacts with C3d in our complex structure.

References and Notes

1. D. T. Fearon, *Semin. Immunol.* **10**, 355 (1998).
2. S. K. A. Law, K. B. M. Reid, *Complement*, in *Focus Series*, D. Male, Ed. (IRL Press, Oxford, UK, ed. 2, 1995).
3. R. H. Carter, D. T. Fearon, *Science* **256**, 105 (1992).
4. S. Moir *et al.*, *J. Exp. Med.* **192**, 637 (2000).
5. J. P. Aubry, S. Pochon, P. Graber, K. U. Jansen, J. Y. Bonnefoy, *Nature* **358**, 505 (1992).
6. J. D. Fingeroth, *et al.*, *Proc. Natl. Acad. Sci. U.S.A.* **81**, 4510 (1984).
7. T. Hebell, J. M. Ahearn, D. T. Fearon, *Science* **254**, 102 (1991).
8. J. M. Ahearn *et al.*, *Immunity* **4**, 251 (1996).
9. H. Molina *et al.*, *Proc. Natl. Acad. Sci. U.S.A.* **93**, 3357 (1996).
10. A. P. Prodeus *et al.*, *Immunity* **9**, 721 (1998).
11. C. A. Lowell *et al.*, *J. Exp. Med.* **170**, 1931 (1989).
12. J. C. Carel, B. L. Myones, B. Frazier, V. M. Holers, *J. Biol. Chem.* **265**, 12293 (1990).
13. A. P. Wiles *et al.*, *J. Mol. Biol.* **272**, 253 (1997).
14. P. N. Barlow *et al.*, *J. Mol. Biol.* **232**, 268 (1993).
15. J. M. Casasnovas, M. Larvie, T. Stehle, *EMBO J.* **18**, 2911 (1999).
16. R. Schwarzenbacher *et al.*, *EMBO J.* **18**, 6228 (1999).
17. CR2 SCR1-2 (residues 20–153) and C3d (residues 995–1303) were expressed in *Pichia pastoris* and in *Escherichia coli*, respectively, and were purified to homogeneity as described in (*29*). Briefly, cells expressing CR2 SCR1-2 were lysed by sonication in 10 mM formate (pH 4.0) buffer, and the supernatant was passed over a SP-Sepharose column (SP HiTrap, Amersham Pharmacia Biotech, Uppsala, Sweden). Eluted CR2 was deglycosylated overnight at 37°C with 33,000 units EndoH per milliliter. The deglycosylated sample was passed over SP-Sepharose again, and a 0.0 to 0.5 M NaCl gradient was used to elute the deglycosylated CR2. C3d was purified from *E. coli* cell lysates using a DEAE column, followed by a MonoQ and then a MonoS column. The interactions of the recombinant CR2 and C3d were studied by Biacore, enzyme-linked immunosorbence assay (ELISA), and analytical ultracentrifugation approaches to confirm the specific binding (*29*). The purified CR2 and C3d were co-crystallized using the method of hanging drop by mixing CR2 and C3d at a molar ratio of approximately 1:1, as determined by careful titration of the two components using native gel shift assay. The total protein concentration (CR2 plus C3d) used for setting up the crystallization drops was approximately 20 mg/ml. The crystallization buffer contained 17% polyethylene glycol (PEG) 2K, 0.2 M zinc acetate, and 0.1 M sodium cacodylate (pH 7.36). Synchrotron data were collected from the crystals at BNL and was processed using D*trek (MSC Inc., Woodlands, TX) (Table 1). The space group is R32, with unit cell $a = b = 170.5$Å, $c = 173.8$ Å. AmoRe (*30*) was used to do molecular replacement that was carried out using C3d (Protein Data Base accession number 1C3D) as a search model. Initial phase improvement was carried out using solvent flattening by the program DM (*30*). Stepwise model building and refinement were carried out using program "O" and CNS (*31*). The final complete model was refined using simulated annealing, positional refinement, and individual B factor refinement. Water molecules were added last using CNS.
18. B. Nagar, R. G. Jones, R. J. Diefenbach, D. E. Isenman, J. M. Rini, *Science* **280**, 1277 (1998).
19. Single-letter abbreviations for the amino acid residues are as follows: A, Ala; C, Cys; D, Asp; E, Glu; F, Phe; G, Gly; H, His; I, Ile; K, Lys; L, Leu; M, Met; N, Asn; P, Pro; Q, Gln; R, Arg; S, Ser; T, Thr; V, Val; W, Trp; and Y, Tyr.
20. Web figure 1 is available at *Science* Online at www.sciencemag.org/cgi/content/full/292/5522/1725/DC1.
21. K. R. Kalli, J. M. Ahearn, D. T. Fearon, *J. Immunol.* **147**, 590 (1991).
22. L. Clemenza, D. E. Isenman, *J. Immunol.* **165**, 3839 (2000).
23. P. J. Bjorkman *et al.*, *Nature* **329**, 512 (1987).
24. C. Branden, J. Tooze, *Introduction to Protein Structure* (Gerland, New York, ed. 2, 1999), p. 16.
25. P. E. Rao, S. D. Wright, E. F. Westberg, G. Goldstein, *Cell. Immunol.* **93**, 549 (1985).
26. H. Molina *et al.*, *J. Immunol.* **154**, 5426 (1995).
27. W. M. Prodinger *et al.*, *J. Immunol.* **161**, 4604 (1998).
28. D. R. Martin, R. L. Marlowe, J. M. Ahearn, *J. Virol.* **68**, 4716 (1994).
29. J. M. Guthridge *et al.*, *Biochemistry*, in press.
30. CCP4, *Acta Crystallogr.* **D50**, 760 (1994).
31. A. T. Brunger *et al.*, *Acta Crystallogr.* **D54**, 905 (1998).

32. M. C. Poznansky, P. M. Clissold, P. J. Lachmann, *J. Immunol.* **143**, 1254 (1989).
33. Supported by Cancer League of Colorado and University of Colorado Cancer Center grants to X.C., NIH R0-1 CA53615 to M.H., and x-ray core facility in the Program in Biomolecular Structure at UCHSC. We thank C. Ogata at X4a and M. Becker at X25 at BNL for assistance in data collection and D. Bain, M. Overduin, L. Chen, S. Perkins, and J. Hannan for discussions. CR2 domain PDB accession number 1GHQ.

18 January 2001; accepted 26 April 2001

Insulin Resistance and a Diabetes Mellitus–Like Syndrome in Mice Lacking the Protein Kinase Akt2 (PKBβ)

Han Cho,[1] James Mu,[2,6] Jason K. Kim,[6,7] Joanne L. Thorvaldsen,[3,6] Qingwei Chu,[2,6] E. Bryan Crenshaw III,[4] Klaus H. Kaestner,[5] Marisa S. Bartolomei,[3,6] Gerald I. Shulman,[6,7] Morris J. Birnbaum[2,6]*

Glucose homeostasis depends on insulin responsiveness in target tissues, most importantly, muscle and liver. The critical initial steps in insulin action include phosphorylation of scaffolding proteins and activation of phosphatidylinositol 3-kinase. These early events lead to activation of the serine-threonine protein kinase Akt, also known as protein kinase B. We show that mice deficient in Akt2 are impaired in the ability of insulin to lower blood glucose because of defects in the action of the hormone on liver and skeletal muscle. These data establish *Akt2* as an essential gene in the maintenance of normal glucose homeostasis.

Type 2 diabetes mellitus is a complex, multisystem disease with a pathophysiology that includes defects in insulin-stimulated peripheral glucose disposal and suppression of hepatic glucose production, as well as in insulin secretion (*1*). Investigations into the molecular pathways that mediate each of these responses in normal individuals has led to the identification of numerous putative signaling molecules, but only a few have been confirmed in vivo as critical to normal glucose homeostasis (*2*). In particular, the in vivo data in support of the insulin receptor, insulin receptor substrate 1 (IRS1) and IRS2, as important to the maintenance of normal insulin responsiveness, have not been matched by equivalent evidence for a physiological role for downstream signaling molecules (*3–6*). The phosphoinositide-dependent serine-threonine protein kinase Akt (also known as protein kinase B, or PKB) has been proposed to be an intermediate in the signaling pathway by which insulin controls both muscle and fat cell glucose uptake as well as hepatic gluconeogenesis (*7–10*). However, experimental approaches based on dominant-inhibitory strategies have yielded contradictory results in regard to a role for Akt in insulin-stimulated glucose uptake, and not all studies have supported the kinase as important to insulin signaling in liver (*11–14*).

In rodents and humans, there are three Akt isoforms, each encoded by a separate gene (*15–17*). Because Akt2 appears to be enriched in insulin-responsive tissues and has been specifically implicated in the metabolic actions of the hormone (*18–20*), we generated mice with a targeted disruption in the *Akt2* locus by homologous recombination. The targeting vector was designed to insert *LoxP* sites (*21*) flanking the sequence containing

[1]Department of Biology, University of Pennsylvania, Philadelphia, PA 19104, USA. [2]Department of Medicine, [3]Department of Cell and Developmental Biology, [4]Department of Neuroscience, and [5]Department of Genetics, University of Pennsylvania School of Medicine, Philadelphia, PA 19104, USA. [6]Howard Hughes Medical Institute and the [7]Department of Internal Medicine, Yale University School of Medicine, New Haven, CT 06520, USA.

*To whom correspondence should be addressed. E-mail: birnbaum@mail.med.upenn.edu

the coding exons 4 and 5 (see supplementary material available on *Science* Online at www.sciencemag.org/cgi/content/full/292/5522/1729/DC1.) (*22*). Mice harboring the targeted allele were identified by Southern blotting and were mated to transgenic mice expressing Cre recombinase driven by a 6-kb 5′-flanking sequence from the *Brn/Pou3f4* gene to cause germ-line excision of exons 4 and 5 (*21*, *23*). The progeny carrying both the *Cre* transgene and the targeted allele were mated with wild-type (WT) mice to obtain offspring in which the *Cre* transgene was segregated away and the targeted allele was excised, as determined by the polymerase chain reaction (PCR) and Southern blotting, respectively. These mice were mated inter se to produce offspring with homozygous deletions of *Akt2*. Western blots of protein extracts prepared from liver, muscle, and isolated adipocytes from homozygous knockout ($Akt2^{-/-}$) mice showed loss of expression of Akt2 (Fig. 1), without detectable effect on the levels of Akt1 or Akt3 (*24*, *25*). Mice from heterozygous matings were born at the expected Mendelian ratio. Newborn pups appeared indistinguishable from their WT littermates and developed into adulthood without apparent growth defects.

Ablation of Akt2 in mice resulted in a mild but statistically significant fasting hyperglycemia (Fig. 2A). The increase in blood glucose concentration in $Akt2^{-/-}$ null animals was more pronounced during fed states (Fig. 2B). Hyperglycemia was accompanied by an increase in the concentration of insulin in serum (Fig. 2C), suggesting that decreased responsiveness to the hormone in peripheral tissues may have resulted in compensatory hyperinsulinemia. Administration of an oral glucose load to 2-month-old $Akt2^{-/-}$ mice revealed mild glucose intolerance compared with WT or heterozygous mice, with elevated blood glucose levels with all time points measured (Fig. 2D). The reduction in blood glucose concentration after intraperitoneal administration of insulin was also impaired in $Akt2^{-/-}$ mice (Fig. 2E), displaying elevated blood glucose at all time points measured (at 60 min; $Akt2^{-/-}$ = 70.8 ± 7.9 mg/dl and WT = 22.3 ± 1.1 mg/dl). In all cases, Akt2 heterozygous mice were indistinguishable from WT mice. These data are consistent with a defect in the actions of insulin on glucose disposal and/or production.

We assessed glucose homoeostasis by infusing into normal and $Akt2^{-/-}$ mice insulin and glucose under conditions that maintained blood glucose concentrations at physiological levels. With the use of such a euglycemic-hyperinsulinemic clamp protocol, total body insulin-dependent glucose disposal can be accurately ascertained, and was found to be reduced in the $Akt2^{-/-}$ mice (Fig. 3A). These data indicate a significant defect in insulin-dependent glucose uptake into hormone-responsive tissues, of which muscle is the most important. To determine if insulin-stimulated glucose uptake is impaired by the loss of Akt2 in skeletal muscles, we assayed uptake of radiolabeled 2-deoxyglucose into isolated muscles in the absence and presence of insulin. We tested two representative muscles that differ in their metabolic properties, the glycolytic extensor digitorum longus (EDL) and oxidative soleus muscles from WT and $Akt2^{-/-}$ mice. Hexose uptake in EDL muscle lacking Akt2 was severely blunted in the presence of 0.33 nM insulin, but the impairment was not apparent on exposure of the muscle to a higher concentration of insulin (Fig. 3B). Deoxyglucose uptake into the soleus muscle lacking Akt2 was not significantly impaired at either the intermediate or maximal concentration of insulin (Fig. 3C). As assessed by Western blotting, targeted disruption of *Akt2* had no effect on the expression of GLUT4, the insulin-responsive glucose transporter in muscle (Fig. 3D) (*26*). Thus, Akt2 is required for the posttranslational events mediating optimal insulin-stimulated glucose uptake, at least in some muscle groups. Insulin-stimulated hexose uptake was also mildly impaired in adipocytes isolated from Akt2-deficent mice (*25*).

In addition to the contribution of reduced insulin responsiveness in muscle to the Type

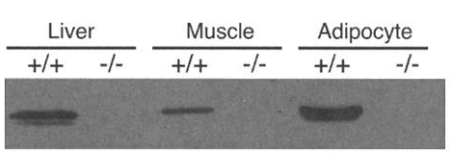

Fig. 1. Analysis of Akt2 expression by Western blot. Homogenates were prepared from liver, skeletal muscle, or adipocytes of $Akt2^{+/+}$ or $Akt2^{-/-}$ mice. Protein (50 μg) was resolved by SDS–polyacrylamide gel electrophoresis (SDS-PAGE) and transferred to a nitrocellulose membrane, which was probed with a polyclonal Akt2 antibody (*20*).

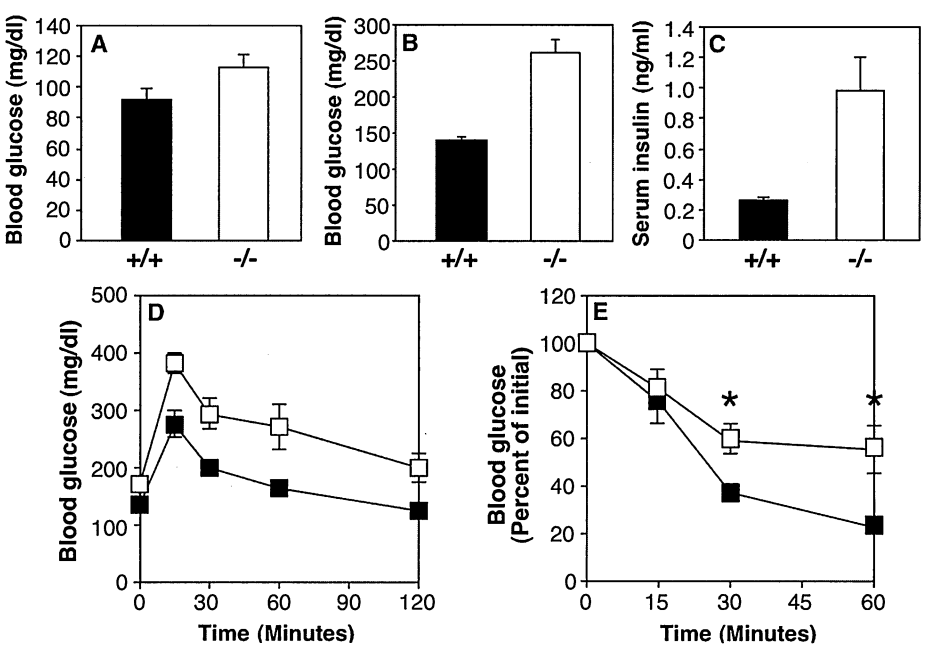

Fig. 2. Altered glucose homeostasis in mice with disruption of the *Akt2* locus. (**A**) Blood glucose concentrations from fasted mice. Values are the mean ± SEM for WT (+/+) mice (solid bar, n = 7 males and 7 females) and $Akt2^{-/-}$ (−/−) mice (open bar; n = 6 males and 6 females; $P < 0.05$, Student's t test). (**B**) Blood glucose concentrations from random-fed mice. Values are the mean ± SEM for WT mice (solid bar, n = 12 males and 12 females) and $Akt2^{-/-}$ mice (open bar, n = 12 males and 11 females; $P < 0.01$, Student's t test). (**C**) Serum insulin concentrations as measured by a rat insulin enzyme-linked immunosorbent assay. Values are the mean ± SEM for WT mice (open bar, n = 7 males and 5 females) and $Akt2^{-/-}$ mice (solid bar; n = 6 males and 4 females; $P < 0.01$, Student's t test). (**D**) Glucose tolerance test. Animals were fasted overnight (15 hours). D-Glucose (2 g/kg) was administered orally to conscious mice, and blood glucose concentrations were sampled at the indicated times. Values are the mean ± SEM for WT mice (solid squares, n = 7 males and 7 females) and $Akt2^{-/-}$ mice (open squares, n = 6 males and 6 females; $P < 0.01$, for WT versus $Akt2^{-/-}$ mice at each time point after the administration of glucose, Student's t test). (**E**) Insulin tolerance test. Porcine insulin (1 U/kg) was administered by intraperitoneal injection to fasted conscious mice and glucose concentrations were determined by a glucometer (Glucometer Elite XL, Bayer, Tarrytown, New York) from whole blood collected from transversely sectioned tails. Values were normalized to the starting glucose concentration at the administration of insulin and represent the mean ± SEM for WT mice (solid squares, n = 3 males and 3 females) and Akt2 KO mice (open squares, n = 3 males and 3 females; asterisk indicates $P < 0.05$, for WT versus $Akt2^{-/-}$ mice, Student's t test).

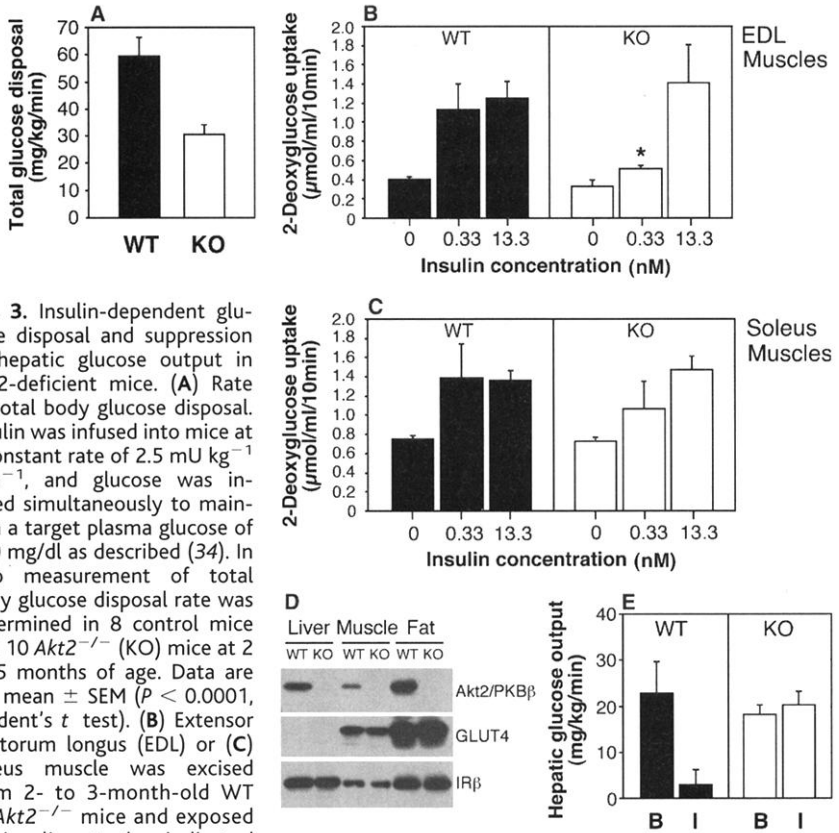

Fig. 3. Insulin-dependent glucose disposal and suppression of hepatic glucose output in Akt2-deficient mice. (**A**) Rate of total body glucose disposal. Insulin was infused into mice at a constant rate of 2.5 mU kg^{-1} min^{-1}, and glucose was infused simultaneously to maintain a target plasma glucose of 140 mg/dl as described (*34*). In vivo measurement of total body glucose disposal rate was determined in 8 control mice and 10 *Akt2*$^{-/-}$ (KO) mice at 2 to 5 months of age. Data are the mean ± SEM ($P < 0.0001$, Student's *t* test). (**B**) Extensor digitorum longus (EDL) or (**C**) soleus muscle was excised from 2- to 3-month-old WT or *Akt2*$^{-/-}$ mice and exposed to insulin at the indicated concentrations. 2-Deoxyglucose uptake was determined as described (*10*). At least six mice per genotype were analyzed. The data are presented as the mean ± SEM and include 2-deoxyglucose uptake from both male and female mice, which did not display sex-dependent differences. In (B), asterisk indicates $P < 0.01$, for glucose uptake in *Akt2*$^{-/-}$ mice versus WT mice, (Student's *t* test). (**D**) Expression of GLUT4 or insulin receptor in *Akt2*$^{-/-}$ mice. Protein extracts from liver, muscle, and fat from WT and *Akt2*$^{-/-}$ mice were resolved by SDS-PAGE and blotted for Akt2, GLUT4, and insulin receptor β-subunit (*20*, *24*, *35*) (**E**) Rate of hepatic glucose output. In vivo hepatic glucose output was deduced by subtracting the glucose infusion rate from the whole-body glucose uptake during hyperinsulinemic-euglycemic clamp, as in (A). B, basal (after overnight fast); and I, insulin stimulated (2.5 mU kg^{-1} min^{-1}). Values are the mean ± SEM for 8 to 10 mice.

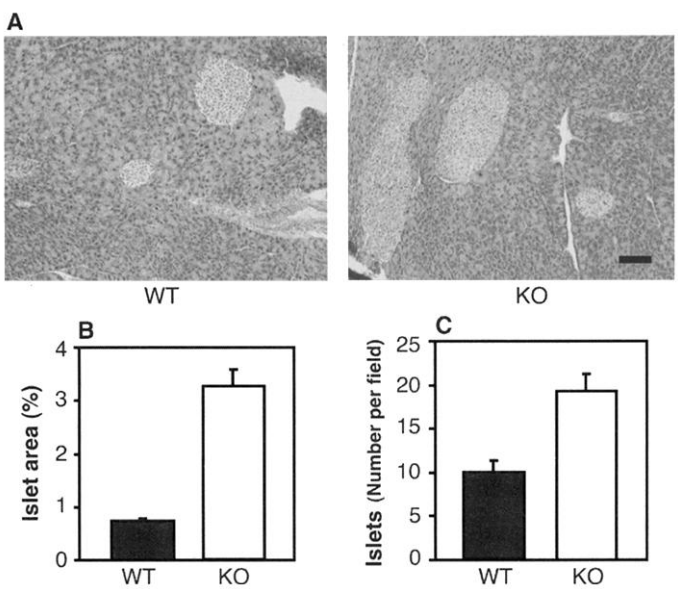

Fig. 4. Analysis of islet mass in pancreata from mice with disruption in the *Akt2* locus. (**A**) Representative islet morphology, shown as hematoxylin and eosin–stained histological sections of pancreata from wild-type (WT) or *Akt2*$^{-/-}$ mice. Bar, represents 100 μm. (**B**) Relative islet area, expressed as a percentage of the total stained pancreatic section, for WT and *Akt2*$^{-/-}$ mice. (**C**) Comparison of islet number. The number of islets per field of view (magnification, ×25) were counted. For (B) and (C), three to five nonoverlapping digital images from three 2- to 3-month-old male mice were used for each genotype. Values are the mean ± SEM. $P < 0.05$, for WT versus Akt2$^{-/-}$ mice (Student's *t* test).

2 diabetic phenotype, recent evidence has emphasized the critical role of hepatic insulin resistance in the development of the disease. For example, muscle-specific insulin receptor knockout mice maintain relatively normal glucose tolerance, suggesting that tissues other than muscle may be critical for maintenance of normal concentrations of circulating glucose (*27*). In support of this idea, insulin fails to suppress hepatic glucose production in mice with a liver-specific insulin receptor knockout, and this targeted genetic defect is associated with severe glucose intolerance (*28*). To determine whether the acute actions of insulin on the liver require Akt2, we measured hepatic glucose output in euglycemic-hyperinsulinemic clamp experiments. Mice lacking Akt2 demonstrated a complete failure of insulin to suppress glucose production normally (Fig. 3E).

A critical factor contributing to whether insulin resistance progresses to diabetes mellitus is the capacity of the pancreatic beta cell to respond to increased demands for insulin secretion. The hyperinsulinemia observed in patients with impaired glucose tolerance is mimicked in mice lacking Akt2 (Fig. 2C). In pancreata from Akt2$^{-/-}$ mice, the near fourfold increase in islet mass is consistent with beta-cell compensation to insulin resistance (Fig. 4, A and B). In spite of the null mutation at the *Akt2* locus, the pancreas remains capable of responding to insulin resistance with an increase in islet mass (Fig. 4B) and number (Fig. 4C). However, because other mouse models of insulin resistance display a greater expansion in beta-cell mass, it is possible that disruption of *Akt2* interferes with the full hyperplasic response (*29*).

On the basis of these data, we conclude that Akt2 is required for the maintenance of normal glucose homeostasis in mice. The phenotype of mice with a monogenic alteration in the *Akt2* locus includes impaired glucose tolerance and mimics some important features of Type 2 diabetes mellitus in humans. The Akt2$^{-/-}$ mice are born without apparent defects, but develop peripheral insulin resistance and nonsuppressible hepatic glucose production accompanied by inadequate compensatory hyperinsulinemia. The results of this study provide definitive in vivo evidence that Akt2, a signaling molecule downstream of the insulin receptor and phosphatidylinositol 3-kinase (PI 3-kinase), is required for the metabolic actions of insulin in liver and contributes to hormone signaling in muscle. The present studies do not allow one to distinguish between primary and secondary effects, so it is possible that the changes in insulin sensitivity in muscle are a result of the compensatory hyperinsulinemia. However, equivalent insensitivity of muscle to insulin is not observed in another model of profound hepatic insulin resistance (*28*), sug-

gesting that the muscle phenotype in the animals lacking Akt2 is a cell-autonomous result of the kinase deficiency in the muscle cell.

Although the simplest interpretation of our findings is that Akt2 represents an obligate intermediate in the pathway by which insulin acutely regulates glucose metabolism in muscle and liver, an alternative possibility is that the long-term absence of Akt2 leads to decreased expression of a critical insulin-signaling molecule. However, the rapidity with which an inducible form of Akt produces insulinlike metabolic effects in both muscle and adipocytes favors the former interpretation (*7*, *30*, *31*). In addition, it is possible that the absence of insulin responsiveness in liver could be secondary to the lack of Akt2 in another tissue. The ability of adipose cell–specific defects to lead to abnormalities in insulin-stimulated glucose uptake in muscle is now well established, and considerable evidence exists in support of an indirect pathway for the regulation of hepatic gluconeogenesis by insulin (*32*, *33*). However, circulating free fatty acid concentrations were normal in the Akt2-deficient mice (*25*). In vivo, the metabolic abnormalities resulting from deficiency of Akt2 are not compensated by the presence of the highly related isoforms, Akt1 (PKBα) or Akt3 (PKBγ). Failure of these Akt isoforms to substitute for Akt2 may reflect differences in substrate specificity, in their relative abundance in insulin-responsive tissues, or both.

References and Notes

1. S. Matthaei, M. Stumvoll, M. Kellerer, H. U. Haring, *Endocr. Rev.* **21**, 585 (2000).
2. T. Kadowaki, *J. Clin. Invest.* **106**, 459 (2000).
3. H. Tamemoto *et al.*, *Nature* **372**, 182 (1994).
4. E. Araki *et al.*, *Nature* **372**, 186 (1994).
5. D. J. Withers *et al.*, *Nature* **391**, 900 (1998).
6. D. Accili *et al.*, *Nature Genet.* **12**, 106 (1996).
7. J. Liao, A. Barthel, K. Nakatani, R. A. Roth, *J. Biol. Chem.* **273**, 27320 (1998).
8. A. D. Kohn, S. A. Summers, M. J. Birnbaum, R. A. Roth, *J. Biol. Chem.* **271**, 31372 (1996).
9. K. Ueki *et al.*, *J. Biol. Chem.* **273**, 5315 (1998).
10. J. T. Brozinick Jr., M. J. Birnbaum, *J. Biol. Chem.* **273**, 14679 (1998).
11. K. Kotani *et al.*, *J. Biol. Chem.* **274**, 21305 (1999).
12. K. Kotani *et al.*, *Mol. Cell. Biol.* **18**, 6971 (1998).
13. Q. Wang *et al.*, *Mol. Cell. Biol.* **19**, 4008 (1999).
14. J. M. Agati, D. Yeagley, P. G. Quinn, *J. Biol. Chem.* **273**, 18751 (1998).
15. D. A. Altomare, C. A. Kozak, G. Sonoda, J. R. Testa, *Cytogenet. Cell Genet.* **74**, 248 (1996).
16. A. Bellacosa *et al.*, *Oncogene* **8**, 745 (1993).
17. S. S. Murthy, A. Tosolini, T. Taguchi, J. R. Testa, *Cytogenet. Cell Genet.* **88**, 38 (2000).
18. M. R. Calera *et al.*, *J. Biol. Chem.* **273**, 7201 (1998).
19. M. M. Hill *et al.*, *Mol. Cell. Biol.* **19**, 7771 (1999).
20. S. A. Summers, E. L. Whiteman, H. Cho, L. Lipfert, M. J. Birnbaum, *J. Biol. Chem.* **274**, 23858 (1999).
21. B. Sauer, *Methods* **14**, 381 (1998).
22. We employed mouse Akt2 specific PCR screening of 129/SvJ mouse genomic **bac**terial artificial chromosome (BAC) library (Genome Systems, St. Louis, MO) to clone the *Akt2* gene. The BAC clone was digested with various restriction enzymes, shotgun subcloned into pBluescript (Stratagene, La Jolla, CA), and screened by hybridization with ^{32}P-labeled human *Akt2* cDNA. The subclones were used to map the mouse *Akt2* locus. PCR-amplified fragments corresponding to recombination arms and floxed sequences were cloned into pFRTLOX (provided by M. A. Magnuson, Vanderbilt University School of Medicine), and linearized with Not I for electroporation into cultured E14 embryonic stem (ES) cells. After selection in G418 and ganciclovir, resistant clones were screened for homologous recombination by Southern blotting of Eco RI–digested genomic DNA and hybridization to Probe 1. Additional hybridization to a fragment within the floxed sequence was performed to ensure recombination upstream of the first LoxP site. To generate chimeric mice, we injected the targeted ES cells into C57Bl/6 blastocysts, which were subsequently implanted into pseudopregnant CD-1 foster mothers by the Transgenic and Chimeric Mouse Facility at the University of Pennsylvania. Resulting chimeric males were mated with C57BL/6 females to obtain agouti pups carrying the targeted allele, as determined by Southern blotting. To remove the floxed sequences, these mice were mated with Cre transgenic mice as described in the text. Transmission of the *Cre* transgene was followed by PCR specific for the transgene. In addition, hybridization of a probe corresponding to the intron between coding exons 4 and 5 was used to confirm the loss of the floxed region.
23. D. Phippard, L. Lu, D. Lee, J. C. Saunders, E. B. Crenshaw III, *J. Neurosci.* **19**, 5980 (1999).
24. For Western blotting, liver, skeletal muscle, and isolated adipocytes or fat pads were homogenized in 50-mM tris buffer (pH 7.5), 1% NP-40, and protease inhibitor cocktail (Sigma, St. Louis, MO) with a Virtishear tissue disrupter. Protein concentration was determined by BCA Protein Assay Kit (Pierce, Rockford, IL) standardized with bovine serum albumin. Total lysate (50 μg) was resolved on SDS–7.5% polyacrylamide gel, and transferred to a nitrocelluose membrane. To detect Akt1, we used affinity-purified antibodies to the COOH-terminus of mouse Akt1, and to detect Glut4, we used affinity purified antibodies to the COOH-terminus of rat GLUT4 was used. Insulin receptor β-subunit was detected with rabbit polyclonal antibody (Santa Cruz, Santa Cruz, CA). Horseradish peroxidase-linked secondary antibody (Santa Cruz) was used for detection by enhanced chemiluminescence. For Northern blotting, 250 to 600 base pairs of 5′-proximal 3′-untranslated sequences to mouse Akt1, Akt2, or Akt3 were random-labeled. Full-length rat Glut4 cDNA was random-labeled for Glut4 expression analysis. Total RNA (10 μg) isolated with TRIZOL Reagent (Gibco-BRL, Grand Island, NY) or mRNA (2 μg) further purified with Oligotex mRNA Kit (Qiagen, Valencia, CA) was submitted to Northern blot analysis by standard techniques.
25. H. Cho, M. J. Birnbaum, unpublished observation.
26. M. J. Birnbaum, *Int. Rev. Cytol.* **137**, 239 (1992).
27. J. C. Bruning *et al.*, *Mol. Cell* **2**, 559 (1998).
28. M. D. Michael *et al.*, *Mol. Cell* **6**, 87 (2000).
29. J. C. Bruning *et al.*, *Cell* **88**, 561 (1997).
30. A. D. Kohn *et al.*, *J. Biol. Chem.* **273**, 11937 (1998).
31. P. B. Iynedjian, R. A. Roth, M. Fleischmann, A. Gjinovci, *Biochem. J.* **351**, 621 (2000).
32. A. D. Cherrington, D. Edgerton, D. K. Sindelar, *Diabetologia* **41**, 987 (1998).
33. E. D. Abel *et al.*, *Nature* **409**, 729 (2001).
34. J. K. Kim, O. Gavrilova, Y. Chen, M. L. Reitman, G. I. Shulman, *J. Biol. Chem.* **275**, 8456 (2000).
35. M. J. Birnbaum, *Cell* **57**, 305 (1989).

36. We thank J. Richa (Transgenic and Chimeric Mouse Facility, University of Pennsylvania) for the generation of chimeric mice and W. Ewens and B. Wolf (University of Pennsylvania) for advice on statistical analyses. The histological procedures were performed by the Center for Molecular Studies in Digestive and Liver Diseases (supported by NIH grant P30 DK50306). Serum insulin was assayed by the Radioimmunoassay Core Facility at the Penn Center for Diabetes (NIH grant P30 19525). H.C. is a recipient of the National Research Service Award for Training in Cell and Molecular Biology (GM07229). Supported in part by NIH grant RO1 DK56886 (to M.J.B.).

19 January 2001; accepted 30 April 2001